

Context-Aware Prompt Tuning for Vision-Language Model with Dual-Alignment

Hongyu Hu^{1,2*}, Tiancheng Lin^{1*}, Jie Wang², Zhenbang Sun², Yi Xu^{1†}

¹Shanghai Jiao Tong University

²ByteDance Inc

mathewcrespo@sjtu.edu.cn

Abstract

Large-scale vision-language models (VLMs), *e.g.*, CLIP, learn broad visual concepts from tedious training data, showing superb generalization ability. Amount of prompt learning methods have been proposed to efficiently adapt the VLMs to downstream tasks with only a few training samples. We introduce a novel method to improve the prompt learning of vision-language models by incorporating pre-trained large language models (LLMs), called **Dual-Aligned Prompt Tuning (DUAL-PT)**. Learnable prompts, like CoOp, implicitly model the context through end-to-end training, which are difficult to control and interpret. While explicit context descriptions generated by LLMs, like GPT-3, can be directly used for zero-shot classification, such prompts are overly relying on LLMs and still underexplored in few-shot domains. With DUAL-PT, we propose to learn more context-aware prompts, benefiting from both explicit and implicit context modeling. To achieve this, we introduce a pre-trained LLM to generate context descriptions, and we encourage the prompts to learn from the LLM’s knowledge by alignment, as well as the alignment between prompts and local image features. Empirically, DUAL-PT achieves superior performance on 11 downstream datasets on few-shot recognition and base-to-new generalization. Hopefully, DUAL-PT can serve as a strong baseline. Code will be available.

Introduction

Pre-trained vision-language models (VLMs), like CLIP (Radford et al. 2021) and ALIGN (Jia et al. 2021), have achieved remarkable success in learning broad visual concepts. These models are trained on web-scale image-text pairs to learn aligned representations of image and text through contrastive loss. By providing specific prompts, *e.g.*, A photo of a {label}, they can be readily applied to downstream tasks in a manner similar to pre-training — calculating the similarities between the task-related descriptions and images encoded by the text and image encoders respectively (Radford et al. 2021).

Despite significant improvements in prompt engineering, classification only based on category names is intuitively insufficient. It overlooks diverse characteristics of categories, resulting in a ‘degradation’ to traditional supervised learning with discrete labels. Moreover, manual design still re-

quires domain expertise, suffers from high variance and inevitably introduces artificial bias, making it a non-trivial task. As a solution, data-driven approaches, *a.k.a.*, the learnable prompts, are introduced to leverage the rich context of additional information for classification. Typical works propose one single prompt (Zhou et al. 2022b), Meta-Net (Zhou et al. 2022a) and prompt sets (Lu et al. 2022; Chen et al. 2023) to implicitly model the class-wise context, instance-specific context and context variance, respectively. While these methods have achieved improved performance, the learned context is not always useful only by a standard classification loss (*e.g.*, the cross-entropy). In some cases, the learned context might coincide with each other and focus on class-agnostic background (Chen et al. 2023). More recently, some works (Menon and Vondrick 2022; Naeem et al. 2023; Pratt, Liu, and Farhadi 2022) turn to the large language models (LLMs), *e.g.*, GPT-3, to explicitly construct context descriptions as prompts, benefiting from the inherent explainability. They hypothesize LLMs possess remarkable world knowledge on a variety of topics. However, a concern with these works is that they may be overly reliant on the pretrained LLMs, which are not always readily available in deployment/inference, particularly for new classes. Moreover, they primarily focus on zero-shot tasks and do not explore the potential of LLMs in few-shot domains. Therefore, we believe a more efficient and effective VLM adaptation should be proposed by making use of both the flexibility of learnable prompts (implicit context modeling) and abundant knowledge of LLMs (explicit context descriptions).

In this work, we propose the context-aware prompt learning approach for VLMs by effectively transferring knowledge from LLMs. Instead of directly using the LLMs for inference, we introduce a powerful LLM as a teacher to generate the class-wise descriptions for knowledge distillation. As is shown in Fig. 1d, the prompts are trained with a dual-alignment strategy that aligns them with both the teacher’s knowledge and local image features. To focus on nuanced and diverse context information, prompts are explicitly constrained to learn from the verbal descriptions from LLM by a distillation loss. Additionally, prompts are aligned with local feature tokens through graph matching, which works on both inter- and intra-domain relations. Only the prompts and the pre-trained VLM are used for downstream task appli-

* Equal contribution.

†Corresponding author.

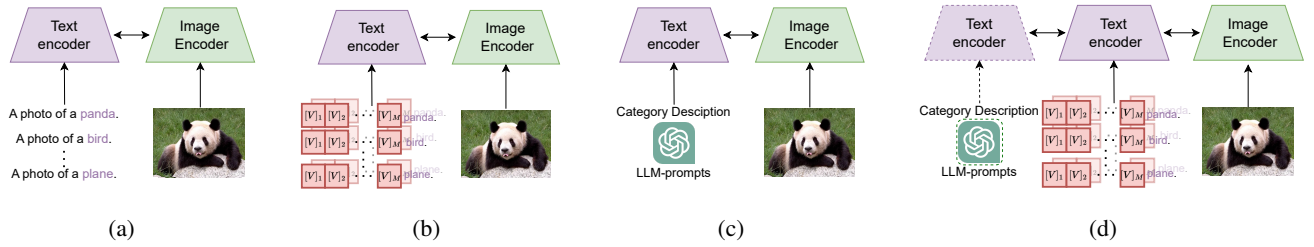


Figure 1: Different paradigms of adapting pre-trained VLM to downstream tasks. (a) Zero-shot inference with manual prompt template. (b) Prompt learning with trainable tokens. (c) Zero-shot inference with class-wise description from LLM. (d) Dual-aligned prompt learning with LLM. Dashed lines indicate that they are only used during the training process.

cations such that no additional inference costs are incurred since the external LLM is not used. This approach not only takes the advantages of both paradigms but also effectively overcomes the limitations mentioned above. Compared with previous methods, the prompts can benefit from both local image features and the LLM’s knowledge. We highlight the following methodological and empirical contributions:

- We propose and formalize a prompt learning method, called DUAL-PT, laying down the first work to bridge the gap between LLM and prompt tuning.
- DUAL-PT is a more efficient and effective way to adapt the VLM (like CLIP) to downstream datasets, making use of both learnable prompts for modelling implicit context and diverse explicit descriptions from LLM.
- With DUAL-PT, prompt tuning is enhanced via the knowledge of LLM, and the potential of LLM in few-shot domains is explored. DUAL-PT is also friendly for inference without access to LLM.
- The proposed method shows superior performance on 11 downstream datasets under few-shot recognition and base-to-new generalization. Further ablation studies and analysis demonstrate the effectiveness of distilling from LLM and graph matching.

Methodology

Preliminaries

Zero-shot inference of CLIP. CLIP (Radford et al. 2021) is a pre-training vision-language model (VLM), consisting of an image encoder $f(\cdot)$ and a text encoder $g(\cdot)$, and the normalized features of the input image \mathbf{x} and text \mathbf{t} are denoted as \mathbf{z} and \mathbf{w} respectively. To perform zero-shot inference on K categories, the prompt templates $\{\mathbf{w}_i\}_{i=1}^K$ are manually designed as “A photo of a {label}”¹. The prediction probability for each downstream category is formulated as:

$$p(y|x) = \frac{\exp(\cos(\mathbf{z}, \mathbf{w}_y)/\tau)}{\sum_{j=1}^K \exp(\cos(\mathbf{z}, \mathbf{w}_j)/\tau)} \quad (1)$$

where τ and $\cos(\cdot)$ are temperature and cosine similarity.

¹For fine-grained classification, it will be “A photo of a {label}, a type of {category}”, e.g., “A photo of a {label}, a type of flower” for Flowers102 (Nilsback and Zisserman 2008).

Prompt Learning. Instead of using pre-defined prompt template, CoOp (Zhou et al. 2022b), for the first time, introduces learnable prompts (prompt tuning) to VLMs. By replacing the pre-defined template with learnable continuous prompt tokens, downstream class descriptions are obtained via concatenating the prompt tokens with the category name. The prediction probability is formulated as:

$$p(y|x) = \frac{\exp(\cos(\mathbf{z}, \mathbf{w}_y(\mathbf{S}))/\tau)}{\sum_{j=1}^K \exp(\cos(\mathbf{z}, \mathbf{w}_j(\mathbf{S}))/\tau)} \quad (2)$$

The prompt \mathbf{S} is optimized by minimizing the cross entropy loss between given label and prompt prediction.

Dual-Aligned Prompt Tuning

The overall framework of the proposed method is shown in Fig. 2. The prompts are optimized by learning from auxiliary LLM and local image features. LLM provides explicit context information by generating detailed class-wise descriptions, which are diverse and fine-grained, corresponding to specific local image features.

Learn From Large Language Model. As is pre-trained with massive corpora, the large language model has readily learned remarkable world knowledge on a variety of topics, and can be considered as external knowledge bases for downstream datasets. Given K categories, we adopt a unified template to query the LLM: Q: What are the useful features for distinguishing a {CLASS} in a photo? Please just give me a list of short phrases. Answer: -², and the answers P would provide diverse local context information for each class:

$$H = \text{LLM}(\text{Questions}) \quad (3)$$

For example, when querying the LLM about {panda}, the LLM would generate the answers like “Black and white fur pattern”, “Round face with black eye patches”, “Round body shape with short legs”, “Distinctive thumb on front paws”, “Large, furry ears”, etc. Then, for each class i , and the context embedding from LLM is formulated as:

$$\mathbf{h}_i = g(H_i) \in R^{e \times d} \quad (4)$$

²“Answer: -” again makes sure the LLM gives a list of descriptions.

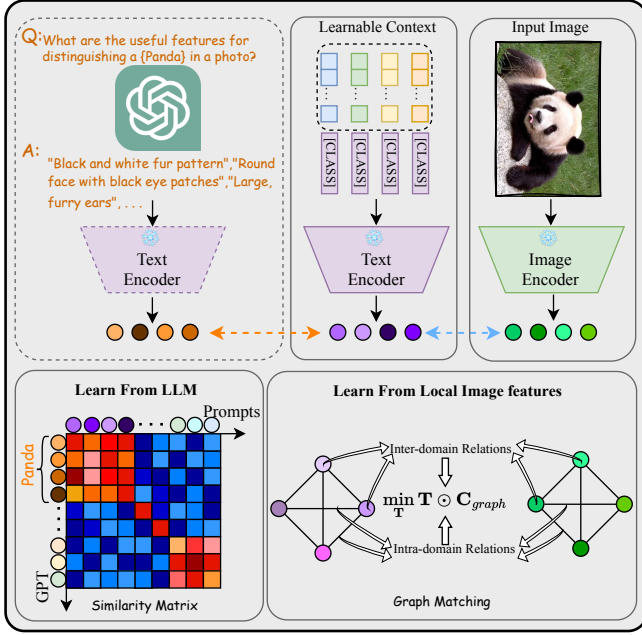


Figure 2: The illustration of DuAL-PT. The prompts are trained in a dual-alignment strategy, with the objective of learning from both the LLM and local images features.

where d is the dimension of embedding, and e represents the number of context information given by LLM.

To distill knowledge from LLM, we set multiple (M) learnable prompts, denoted as $\mathbf{w}_i(\mathbf{S}) \in \mathbb{R}^{M \times d}$, and align the prompts with these explicit descriptions of the corresponding category generated by LLM. Cosine distance is applied as a regularization to guide the prompts to be close to their corresponding class-wise descriptions in the embedding space, and the overall distillation loss for all categories is demonstrated as:

$$L_{\text{LLM}} = \frac{1}{K} \sum^K 1 - \cos(\mathbf{w}_i(\mathbf{S}), \mathbf{h}_i) \quad (5)$$

Note that there is also other implementation of the distillation, which is discussed in the ablation studies.

Learn from local image features. We aim to align the multiple prompts with the local image features instead of the global one. The core idea is that each context description generated by LLM only focuses on a specific pattern within a class. Aligning prompts in this way will encourage the model to concentrate on diverse visual features important for fine-grained classification. We define it as a graph matching problem, where node and edge matching capture inter- and intra-domain relations, respectively. Inter-domain relations facilitate the distribution alignment between the prompts with image features, while the intra-domain relations are motivated by the fact that local image features are highly-related rather than being independent.

Given local image feature vectors $\mathbf{Z} \in \mathbb{R}^{N \times d}$, we construct a graph $G_{\text{img}}(V_{\text{img}}, E_{\text{img}})$, with V_{img} and E_{img} as

Algorithm 1: Solve Assignment Matrix.

Require: Local feature $\{\mathbf{z}_i\}_{i=1}^N$, prompts $\{\mathbf{w}_j\}_{j=1}^M$, vector \mathbf{p}, \mathbf{q} , regularization λ

- 1: $\mathbf{C}_{WD} = 1 - \cos(\mathbf{Z}, \mathbf{W})$
- 2: $\mathbf{C}_z = \cos(\mathbf{Z}, \mathbf{Z}), \mathbf{C}_w = \cos(\mathbf{W}, \mathbf{W})$
- 3: $\mathbf{C}_{zw} = \mathbf{C}_z^2 \mathbf{p} \mathbf{1}_M^\top + \mathbf{1}_N \mathbf{q} (\mathbf{C}_w^2)^\top$
- 4: **for** $i = 1, 2, 3, \dots$ **do**
- 5: $\mathbf{C}_{GWD} = \mathbf{C}_{zw} - 2\mathbf{C}_z \mathbf{T} \mathbf{C}_w^\top$
- 6: $\mathbf{C}_{graph} = \alpha \mathbf{C}_{GWD} + (1 - \alpha) \mathbf{C}_{WD}$
- 7: $\mathbf{a} = \mathbf{1}, \mathbf{K} = \exp(-\mathbf{C}_{graph} / \lambda)$
- 8: **for** $j = 1, 2, 3, \dots$ **do**
- 9: $\mathbf{a} = \mathbf{p} / \mathbf{K} \mathbf{b}, \mathbf{b} = \mathbf{q} / \mathbf{K}^\top \mathbf{a}$
- 10: **end for**
- 11: $\mathbf{T} = \text{diag}(\mathbf{a}) \mathbf{K} \text{diag}(\mathbf{b})$
- 12: **end for**

nodes and edges. To fully explore the relations among local features, the graph is fully connected with cosine similarity as edge weights. Similarly, the graph for prompts $G_{\text{text}}(V_{\text{text}}, E_{\text{text}})$ is constructed in the same manner. We now look into a unified method for aligning the two relations across domain.

We first investigate how prompts are directly corresponding to local visual features. Wasserstein Distance (WD) is a common metric to compare the distributions. Given the cost function \mathbf{C}_{WD} between local visual features and prompts, solving WD in eq. (6) learns an assignment plan \mathbf{T} for inter-domain alignment.

$$D_w(\mathbf{Z}, \mathbf{W}) = \min_{\mathbf{T}} \mathbf{T} \odot \mathbf{C}_{WD} \quad (6)$$

where cosine distance $[\mathbf{C}_{WD}]_{ij} = 1 - \cos(\mathbf{z}_i, \mathbf{w}_j)$ is set as the cost function in our case, \odot denotes Hadamard product.

As is figured out before, intra-domain relation is also essential for downstream task. We propose to align the edges to maintain this relation. We aim to match the intra-domain relations between local visual features and prompt embedding. It is implemented with Gromov-Wasserstein Distance (GWD), which operates on the distance between pairs of entities calculated within the domain and measures how these distances compare to those in another domain. Solving GWD gives another plan for aligning two domains for intra-domain relation. Following (Alvarez-Melis and Jaakkola 2018; Peyré, Cuturi, and Solomon 2016), it is defined as:

$$\begin{aligned} D_{gw}(\mathbf{Z}, \mathbf{W}) &= \min_{\mathbf{T}} \mathbf{T} \odot \mathbf{C}_{GWD} \\ &= \min_{\mathbf{T}} \mathbf{T} \odot (\mathbf{C}_{zw} - 2\mathbf{C}_z \mathbf{T} \mathbf{C}_w^\top) \end{aligned} \quad (7)$$

where $\mathbf{C}_z = \cos(\mathbf{Z}, \mathbf{Z}), \mathbf{C}_w = \cos(\mathbf{W}, \mathbf{W})$ denote intra-domain similarities and $\mathbf{C}_{zw} = \mathbf{C}_z^2 \mathbf{p} \mathbf{1}_M^\top + \mathbf{1}_N \mathbf{C}_w \mathbf{q} (\mathbf{C}_w^2)^\top$ represent cross-domain similarities (\mathbf{p}, \mathbf{q} are possibility vectors with uniform weights, i.e., $\mathbf{p}_i = \frac{1}{M}, \mathbf{q}_i = \frac{1}{N}$)

Aligning the two domains with graph matching should consider these two relations at the same time. Therefore, we

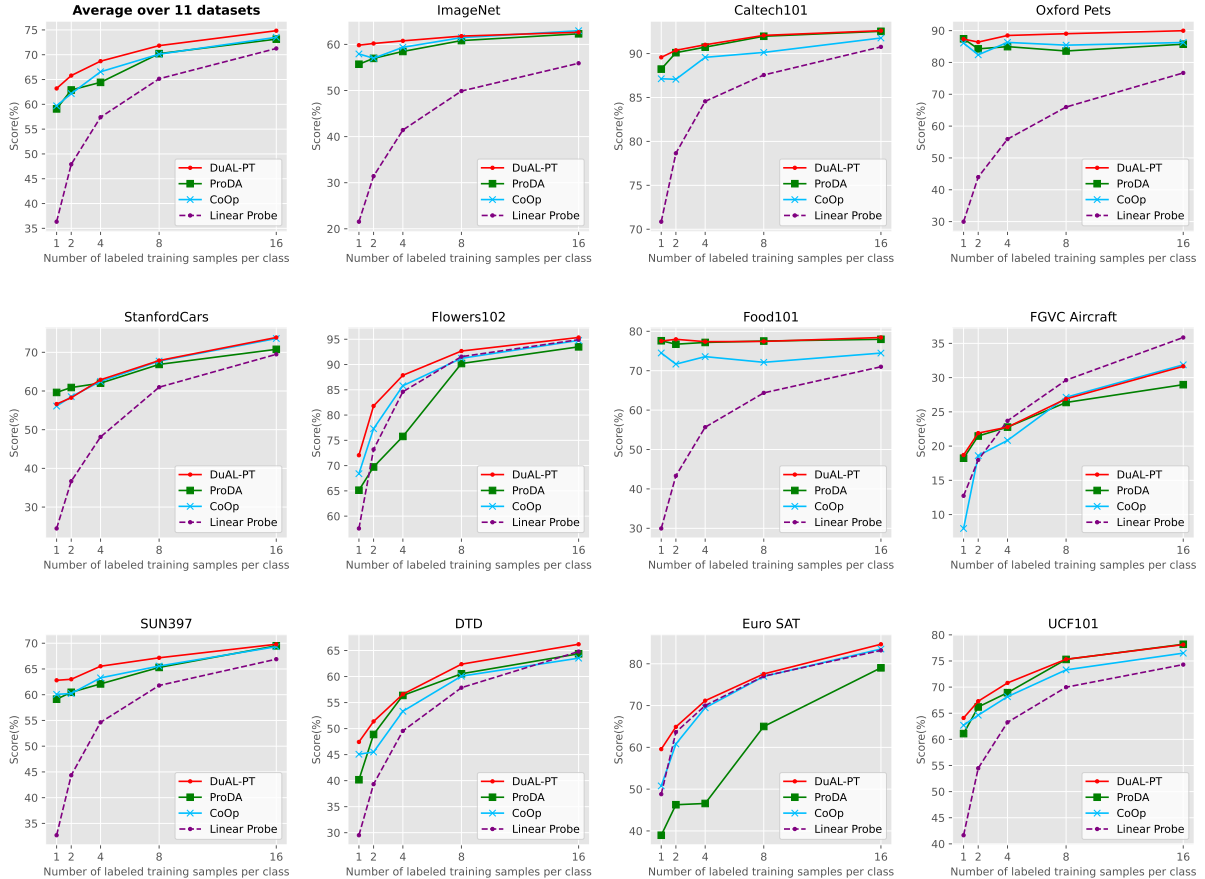


Figure 3: Results of few-shot learning on 11 downstream datasets. The proposed method outperforms others in general.

combine C_{WD} and C_{GWD} with a weighting parameter α as an overall, and the final assignment matrix is solved with Sinkhorn-Knopp algorithm (Cuturi 2013). The complete solution to graph matching is shown in Algorithm 1.

Training Objective. The obtained assignment matrix \mathbf{T} shows how the local visual features and prompts are related, which is further interpreted as the weights to ensemble various prompts. We formulate the prediction probability in Eq.8:

$$p(y = k|x) = \frac{\exp(\mathbf{T} \odot (\mathbf{z}\mathbf{w}(k))/\tau)}{\sum_{k'} \exp(\mathbf{T} \odot (\mathbf{z}\mathbf{w}(k')/\tau)} \quad (8)$$

Implicit context information is learned by applying cross-entropy loss L_{img} with $p(y = k|x)$ and the label.

To learn from LLM and local image features for more diverse context, the overall loss function is demonstrated in Eq.9, with β to balance the dual alignment:

$$L = \beta L_{\text{LLM}} + (1 - \beta) L_{\text{img}} \quad (9)$$

Inference. Only the prediction $p(y = k|x)$ will be counted for downstream inference. Without further access to external LLM, the proposed method is friendly to deployment, and can be easily adapted to unseen categories.

Experiments

Datasets. Following CoOp (Zhou et al. 2022b), we evaluate the proposed method on 11 downstream datasets, including ImageNet (Deng et al. 2009), Caltech101 (Fei-Fei, Fergus, and Perona 2004), OxfordPets (Parkhi et al. 2012), StanfordCars (Krause et al. 2013), Flowers102 (Nilsback and Zisserman 2008), Food101 (Bossard, Guillaumin, and Van Gool 2014), FGVC Aircraft (Maji et al. 2013), SUN397 (Xiao et al. 2010), DTD (Cimpoi et al. 2014), EuroSAT (Helber et al. 2019), and UCF101 (Soomro, Zamir, and Shah 2012). Dataset details are provided in the supplementary materials.

Evaluation Protocol. We evaluate the proposed method under few-shot learning and base-to-new generalization. For few-shot learning, the prompt is trained on 1,2,4,8,16 shots in each class, and tests on the complete validation set. For base-to-new generalization, the prompt is trained with 16 samples per category on base classes and tested on new classes. We report the average results over 3 random seeds.

Baseline Methods. For few-shot learning, we compare DuAL-PT with CoOp (Zhou et al. 2022b), ProDA (Lu et al. 2022), and linear probe CLIP (Radford et al. 2021). CoOp is pioneering in prompt learning, while ProDA learns diverse prompts from distributions. These methods are com-

Table 1: Comparison of CoCoOp and CoDUAL-PT (conditional DUAL-PT) in base-to-new generalization. **H**: Harmonic mean.

(a) Average.			(b) ImageNet.			(c) Caltech101			(d) OxfordPets						
Base	New	H	Base	New	H	Base	New	H	Base	New	H				
CoCoOp	75.10	63.73	67.84	CoCoOp	68.30	62.80	65.43	CoCoOp	94.35	89.77	92.00	CoCoOp	92.40	96.07	94.19
CoDUAL-PT	75.50	66.09	69.95	CoDUAL-PT	68.42	62.17	65.15	CoDUAL-PT	95.00	90.17	92.52	CoDUAL-PT	92.60	94.80	93.69
(e) StanfordCars.			(f) Flowers102.			(g) Food101.			(h) FGVCaircraft.						
Base	New	H	Base	New	H	Base	New	H	Base	New	H				
CoCoOp	63.63	64.50	64.06	CoCoOp	89.43	67.60	76.99	CoCoOp	83.40	83.60	83.50	CoCoOp	22.87	16.17	18.95
CoDUAL-PT	63.63	65.46	64.53	CoDUAL-PT	89.50	67.77	77.13	CoDUAL-PT	83.83	84.40	84.11	CoDUAL-PT	24.07	21.83	22.89
(i) SUN397.			(j) DTD.			(k) EuroSAT.			(l) UCF101.						
Base	New	H	Base	New	H	Base	New	H	Base	New	H				
CoCoOp	74.37	73.40	73.88	CoCoOp	71.83	46.37	56.35	CoCoOp	88.50	34.47	49.62	CoCoOp	77.00	66.30	71.25
CoDUAL-PT	74.47	73.70	74.08	CoDUAL-PT	73.13	49.13	58.77	CoDUAL-PT	88.70	51.97	65.54	CoDUAL-PT	77.10	67.40	71.92

petitive in our community. For base-to-new generalization, CoCoOp (Zhou et al. 2022a) is a strong baseline work.

Implementation Details. Following the widely-used experimental settings in CoOp, ResNet50 (He et al. 2016) pre-trained with CLIP is selected as the image encoder. The local feature map obtained from the last pooling layer has a size of 7×7 . The number of local prompts is set as 4 in our experiments. We adopt GPT-3.5 (Radford et al. 2018) with a temperature of 0.7 to generate local visual context. The scaling factor α in graph matching and the weight β for L_{LLM} are both 0.2. We train the prompts with SGD optimizer with an initial learning rate of 0.002, which decays by the cosine annealing rule. The maximum epoch is 50 for 1 shot, 100 for 2/4 shots, 200 for 8/16 shots, and 10 for base-to-new generalization. Note that DUAL-PT has 4 prompts rather than 1, we improve the length of learnable tokens from 16 to 64 in CoOp to reach the same number of trainable parameters for fair comparison.

Few-Shot Learning

Fig. 3 shows the comparison with the baseline methods on 11 downstream datasets. We notice that DUAL-PT surpasses CoOp (blue) on most datasets, validating the idea of learning enriched context from LLM and local image features. Moreover, compared with ProDA (green), our method is more robust on downstream datasets. Also working on diverse prompts for more context, ProDA fails to achieve promising results on datasets like Flowers102 and EuroSAT, while the proposed method is capable of handling such a fine-grained task, which demonstrates that DUAL-PT manages to learn evident context from the LLM. In general, the proposed method surpasses the baselines by 3.49%, 3.60%, 2.10%, 1.73%, and 1.33% on 1/2/4/8/16 shots in average over all datasets.

Base-to-New Generalization

We further apply DUAL-PT to a conditional setting to evaluate how well the proposed method can generalize to new classes. For implementation, following CoCoOp, we build a meta net to generate for each input a conditional token,

which is then combined with the context vector as an image-specific prompt. Table 1 shows that CoDUAL-PT outperforms CoCoOp on most datasets, especially on FGVCaircraft, DTD and EuroSAT, where fine-grained context is important. Generally, DUAL-PT improves the baseline by 0.40% , 2.36%, 2.11% in base, new and Harmonic. Moreover, without access to LLM when inference on new classes, the proposed DUAL-PT outperforms the baseline by a large margin, further demonstrating that the prompts have learned broad class-wise context for generalization.

Ablation Study and Further Discussion

We conduct more ablation studies on Caltech101, DTD. These two datasets cover general and fine-grained recognition tasks, thus are representative to investigate the effectiveness the components.

How to distill from LLM? As LLM provides enriched context information beneficial for visual recognition, learning from LLM is of great significance.

Dataset	Loss	Shot1	Shot2	Shot4	Shot8	Shot16
Caltech	WD	89.50	90.27	90.87	91.63	92.50
	CE	87.37	89.27	90.27	90.27	91.00
	Cosine	89.57	90.37	91.00	91.33	92.43
DTD	WD	47.03	51.37	54.83	62.27	66.37
	CE	45.23	49.63	53.83	60.00	63.70
	Cosine	47.43	51.37	56.60	62.37	66.20

We investigate Wasserstein Distance (WD), instance-wise cross-entropy (CE) and the adopted cosine distance (Cosine). WD and Cosine both work on class-wise distillation, dependent of input samples. Such a soft regularization achieves comparable but promising performance. CE is an instance-wise supervision, however, falls behind from the other two. We infer that instance-wise logits are noisy for learning class-wise knowledge. We adopt cosine distance by default, considering the computational cost of WD.

Other alternatives to learn context information? LLM provides external context from a language’s perspective. Table. 2 demonstrates other two methods to learn context. CAM (Class Activation Map) explicitly highlights the regions of interest, thus offers more context information from visual domain. Sim calculates the importance of local feature tokens with the global token, and only top 50% tokens

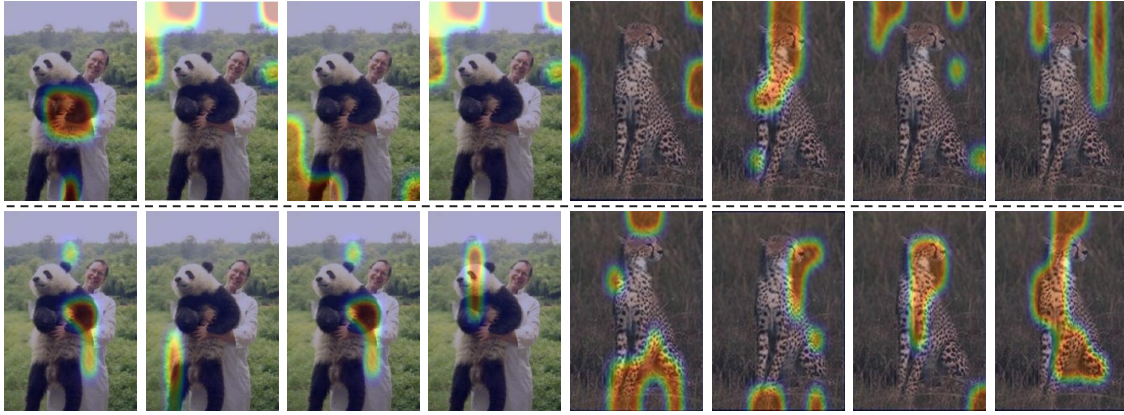


Figure 4: Visualization of the learned prompts. Aligned **without** (1st row) v.s. **with** LLM (2nd row) .

Table 2: Ablation Studies on different implementation and other alternatives of the components.

Dataset	Context	Align	Shot1	Shot2	Shot4	Shot8	Shot16
Caltech101	None	Graph	88.37	87.57	89.20	89.20	92.37
	CAM	Graph	88.90	87.67	89.43	90.70	92.57
	SIM	Graph	88.57	87.73	89.40	90.67	92.43
	GPT	Attn	87.73	88.30	89.47	89.63	91.83
	GPT	Node	89.37	90.00	90.10	90.67	92.43
	GPT	Edge	88.90	89.80	90.27	91.27	91.83
	GPT	Graph	89.57	90.37	91.00	91.33	92.43
DTD	None	Graph	46.43	50.27	55.93	61.30	64.80
	CAM	Graph	47.00	51.03	56.50	61.47	65.10
	SIM	Graph	47.03	50.20	56.50	60.60	64.57
	GPT	Attn	43.33	46.40	53.13	59.67	62.83
	GPT	Node	46.83	51.53	54.63	61.30	65.23
	GPT	Edge	47.03	51.10	54.57	61.80	65.40
	GPT	Graph	47.43	51.37	56.60	62.37	66.20

are selected to contribute to final classification result. This strategy filters out irrelevant regions, giving local context from a feature’s perspective. Experimental results show that learning from LLM achieves the best performance. We infer that **CAM** gives instance-wise context, which is not general within the class, and similarity with global representation (**Sim**) cannot explicitly represent fine-grained variance.

How does LLM benefit prompt learning? As is shown in Table 2, LLM improves few-shot recognition by 1.20%, 2.80%, 1.80%, 2.13%, and 0.06% on Caltech, 1.00%, 1.10%, 0.67%, 1.07%, and 1.40% on DTD (GPT + Graph vs None + Graph). Fig. 4 further shows that, with the guidance of LLM, prompts are learned to focus more on the key visual features, demonstrating the effectiveness of the LLM.

How to align multiple prompts? Considering both inter- and intra- domain relationships, we construct a graph in each domain and align the domains by matching graphs. Applying cross-attention (**Attn**) to generate a dense mapping function is a simple and direct idea. However, it is shown in Table 2 that cross-attention alignment achieves the poorest performance. Essentially, it only obtains the alignment relations with feature similarity, ignoring more comprehensive relations. Moreover, capturing inter- and intra-relations is mutually beneficial to few-shot recognition, demonstrating

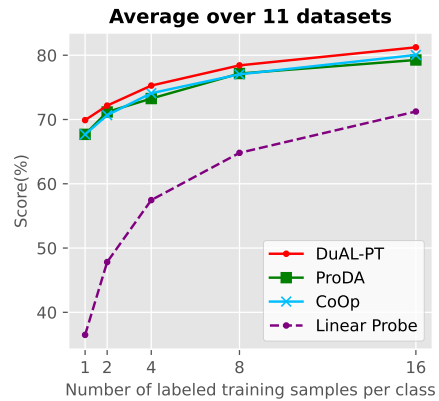


Figure 5: Few-shot recognition on 11 datasets with ViT.

that it is practical to align prompts and local features with graph. (**Graph vs Node/Edge**).

How does DUAL-PT work on ViT? More experiments are conducted on CLIP-ViT-B/16 backbone. Fig.5 shows that DUAL-PT outperforms other methods over 2.22%, 0.99%, 2.02%, 1.27%, 1.97% on 1/2/4/8/16 shots on average over all datasets. Working on different backbones, DUAL-PT can consistently outperform other methods, demonstrating the effectiveness and generalization ability of DUAL-PT.

Number of local prompts. We study the number M of local prompts to align with the local image features and LLM descriptions under the setting of few-shot learning. Figs. 6a and 6b show that more local prompts are potentially beneficial, while there is no obvious improvement when $M > 4$ on DTD. Considering computation and time consumption, we set M as 4 in main experiments as a trade-off solution.

Balancing learning from LLM and local image features. The prompts are trained with a dual-alignment strategy, and we further investigate the scaling factor to balance different branches. Fig. 6c demonstrates that distilling from LLM benefits downstream classification, and soft regularization for this branch with less weight achieves better results.

Balancing edge and node in graph match. we match two

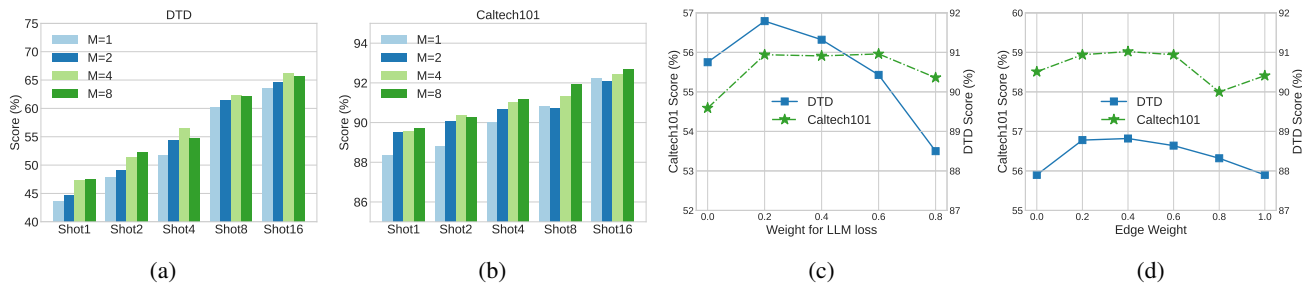


Figure 6: Ablation study on the hyper-parameters. (a)(b) Number of local prompts. (c) Weight for LLM loss in the dual-alignment strategy. (Average of 1/2/4/8/16 shots) (d) Edge weight in graph match. (Average of 1/2/4/8/16 shots)

graphs by combining the cost function of WD and GWD. We ablate the weight α of the GWD (edge) cost function. The results in Fig. 6d reveal that setting α as 0.2 achieves promising results in both datasets. Notably, if two graphs are matched by the edge or node alone ($\alpha = 0/1$), the overall performance drops, indicating inter- and intra- relationships are mutually beneficial for learning good prompts.

Analysis of inference time. Compared with CoOp, DUAL-PT requires 10% extra time. It mainly comes from graph matching, which is of $O(N^4)$ time complexity ($N=4$ in DUAL-PT). Given the gain, little extra time is acceptable.

Related Works

Vision-Language Pre-training

Vision-language models are capable of learning broad and generic visual concepts, showing promising generalization ability to a large variety of downstream tasks and datasets. With the objective of learning the connection between visual content and language, a large number of early works aim to learn representations by predicting the captions of images (Desai and Johnson 2021; Li et al. 2017; Radford et al. 2019; Sariyildiz, Perez, and Larlus 2020). However, the main obstacle is that these models are trained on relatively small datasets, e.g., Flickr (Joulin et al. 2016) and COCO Captions (Desai and Johnson 2021). Recent vision-language models based on contrastive learning have shown superb results, benefiting from web-scale image-text pairs. In particular, CLIP (Radford et al. 2021) and ALIGN (Jia et al. 2021), aim to learn the aligned representations of image and text by contrastive loss. Later representative works like ALBEF (Li et al. 2021) and BLIP (Li et al. 2022) integrate contrastive loss with other pretext tasks for better pre-training and empower the transferability of VLM.

Prompt Learning

Inspired by the success of *prompt* in the NLP domain, numerous studies introduce prompt learning to better adapt the pre-trained CLIP to downstream datasets, and the core idea is to align learnable prompts with image representations. CoOp (Zhou et al. 2022b) is the pioneer work in this field. It optimizes continuous prompts by minimizing the classification loss on target datasets, and achieves promising results in adapting pre-trained models to downstream few-shot recognition task. Based on CoOp, more recent works like

CoCoOp (Zhou et al. 2022a) and ProDA (Lu et al. 2022) aim at better generalization by aligning visual representation with image-specific prompts or the distribution of diverse prompts. However, the learned context is not always useful only by a standard classification loss with the category name, which motivates us to query the powerful large language model to access abundant knowledge.

Large Language Model for Image Classification

LLMs like GPT-3 (Brown et al. 2020), OPT (Zhang et al. 2022), and PaLM (Chowdhery et al. 2022) are trained on massive web-scale corpora, showing impressive abilities towards downstream zero-shot and few-shot scenarios such as open-vocabulary question and answering. Some recent works apply LLM as a powerful knowledge base to facilitate image classification task. I2MVFormer (Naeem et al. 2023) learns multi-view semantic embeddings from LLM to boost zero-shot classification. Sachit *et al.* (Menon and Vondrick 2022) query the LLM for descriptive features of each class, which improves the model’s generalization. However, these works overly rely on the external LLM, which is not always available in deployment/inference. Furthermore, descriptions from LLM are only tested for zero-shot scenarios, leaving the potential for few-shot learning unexplored.

Conclusion

Various prompt learning methods have been developed to better transfer the pre-trained vision-language model to downstream recognition tasks. This paper proposes a novel prompt tuning method, namely Dual-ALigned Prompt Tuning (DUAL-PT), where prompts are aligned with powerful large language model and local image features. As the first work to bridge the gap between LLMs and prompt learning, DUAL-PT provides fresh insight into prompt engineering problem. Comprehensive experiments have been conducted on downstream tasks, and the results reveal that DUAL-PT is capable of further improving the transferability of the vision-language model via distilling from LLM. In future, with the advances of LLMs, DUAL-PT is expected to work better by learning from a stronger teacher. We also plan to bridge the LLMs with prompt learning in a more elegant manner.

References

- Alvarez-Melis, D.; and Jaakkola, T. S. 2018. Gromov-Wasserstein alignment of word embedding spaces. *arXiv preprint arXiv:1809.00013*.
- Bossard, L.; Guillaumin, M.; and Van Gool, L. 2014. Food-101—mining discriminative components with random forests. In *Computer Vision—ECCV 2014: 13th European Conference, Zurich, Switzerland, September 6–12, 2014, Proceedings, Part VI 13*, 446–461. Springer.
- Brown, T.; Mann, B.; Ryder, N.; Subbiah, M.; Kaplan, J. D.; Dhariwal, P.; Neelakantan, A.; Shyam, P.; Sastry, G.; Askell, A.; et al. 2020. Language models are few-shot learners. *Advances in neural information processing systems*, 33: 1877–1901.
- Chen, G.; Yao, W.; Song, X.; Li, X.; Rao, Y.; and Zhang, K. 2023. PLOT: Prompt Learning with Optimal Transport for Vision-Language Models. In *The Eleventh International Conference on Learning Representations*.
- Chowdhery, A.; Narang, S.; Devlin, J.; Bosma, M.; Mishra, G.; Roberts, A.; Barham, P.; Chung, H. W.; Sutton, C.; Gehrmann, S.; et al. 2022. Palm: Scaling language modeling with pathways. *arXiv preprint arXiv:2204.02311*.
- Cimpoi, M.; Maji, S.; Kokkinos, I.; Mohamed, S.; and Vedaldi, A. 2014. Describing textures in the wild. In *Proceedings of the IEEE conference on computer vision and pattern recognition*, 3606–3613.
- Cuturi, M. 2013. Sinkhorn distances: Lightspeed computation of optimal transport. *Advances in neural information processing systems*, 26.
- Deng, J.; Dong, W.; Socher, R.; Li, L.-J.; Li, K.; and Fei-Fei, L. 2009. Imagenet: A large-scale hierarchical image database. In *2009 IEEE conference on computer vision and pattern recognition*, 248–255. Ieee.
- Desai, K.; and Johnson, J. 2021. Virtex: Learning visual representations from textual annotations. In *Proceedings of the IEEE/CVF conference on computer vision and pattern recognition*, 11162–11173.
- Fei-Fei, L.; Fergus, R.; and Perona, P. 2004. Learning generative visual models from few training examples: An incremental bayesian approach tested on 101 object categories. In *2004 conference on computer vision and pattern recognition workshop*, 178–178. IEEE.
- He, K.; Zhang, X.; Ren, S.; and Sun, J. 2016. Deep residual learning for image recognition. In *Proceedings of the IEEE conference on computer vision and pattern recognition*, 770–778.
- Helber, P.; Bischke, B.; Dengel, A.; and Borth, D. 2019. Eurosat: A novel dataset and deep learning benchmark for land use and land cover classification. *IEEE Journal of Selected Topics in Applied Earth Observations and Remote Sensing*, 12(7): 2217–2226.
- Jia, C.; Yang, Y.; Xia, Y.; Chen, Y.-T.; Parekh, Z.; Pham, H.; Le, Q.; Sung, Y.-H.; Li, Z.; and Duerig, T. 2021. Scaling up visual and vision-language representation learning with noisy text supervision. In *International Conference on Machine Learning*, 4904–4916. PMLR.
- Joulin, A.; Van Der Maaten, L.; Jabri, A.; and Vasilache, N. 2016. Learning visual features from large weakly supervised data. In *Computer Vision—ECCV 2016: 14th European Conference, Amsterdam, The Netherlands, October 11–14, 2016, Proceedings, Part VII 14*, 67–84. Springer.
- Krause, J.; Stark, M.; Deng, J.; and Fei-Fei, L. 2013. 3d object representations for fine-grained categorization. In *Proceedings of the IEEE international conference on computer vision workshops*, 554–561.
- Li, A.; Jabri, A.; Joulin, A.; and Van Der Maaten, L. 2017. Learning visual n-grams from web data. In *Proceedings of the IEEE International Conference on Computer Vision*, 4183–4192.
- Li, J.; Li, D.; Xiong, C.; and Hoi, S. 2022. Blip: Bootstrapping language-image pre-training for unified vision-language understanding and generation. In *International Conference on Machine Learning*, 12888–12900. PMLR.
- Li, J.; Selvaraju, R.; Gotmare, A.; Joty, S.; Xiong, C.; and Hoi, S. C. H. 2021. Align before fuse: Vision and language representation learning with momentum distillation. *Advances in neural information processing systems*, 34: 9694–9705.
- Lu, Y.; Liu, J.; Zhang, Y.; Liu, Y.; and Tian, X. 2022. Prompt distribution learning. In *Proceedings of the IEEE/CVF Conference on Computer Vision and Pattern Recognition*, 5206–5215.
- Maji, S.; Rahtu, E.; Kannala, J.; Blaschko, M.; and Vedaldi, A. 2013. Fine-grained visual classification of aircraft. *arXiv preprint arXiv:1306.5151*.
- Menon, S.; and Vondrick, C. 2022. Visual classification via description from large language models. *arXiv preprint arXiv:2210.07183*.
- Naeem, M. F.; Khan, M. G. Z. A.; Xian, Y.; Afzal, M. Z.; Stricker, D.; Van Gool, L.; and Tombari, F. 2023. I2MVFormer: Large Language Model Generated Multi-View Document Supervision for Zero-Shot Image Classification. In *Proceedings of the IEEE/CVF Conference on Computer Vision and Pattern Recognition*, 15169–15179.
- Nilsback, M.-E.; and Zisserman, A. 2008. Automated flower classification over a large number of classes. In *2008 Sixth Indian Conference on Computer Vision, Graphics & Image Processing*, 722–729. IEEE.
- Parkhi, O. M.; Vedaldi, A.; Zisserman, A.; and Jawahar, C. 2012. Cats and dogs. In *2012 IEEE conference on computer vision and pattern recognition*, 3498–3505. IEEE.
- Peyré, G.; Cuturi, M.; and Solomon, J. 2016. Gromov-Wasserstein Averaging of Kernel and Distance Matrices. In Balcan, M. F.; and Weinberger, K. Q., eds., *Proceedings of The 33rd International Conference on Machine Learning*, volume 48 of *Proceedings of Machine Learning Research*, 2664–2672. New York, New York, USA: PMLR.
- Pratt, S.; Liu, R.; and Farhadi, A. 2022. What does a platypus look like? generating customized prompts for zero-shot image classification. *arXiv preprint arXiv:2209.03320*.
- Radford, A.; Kim, J. W.; Hallacy, C.; Ramesh, A.; Goh, G.; Agarwal, S.; Sastry, G.; Askell, A.; Mishkin, P.; Clark, J.;

et al. 2021. Learning transferable visual models from natural language supervision. In *International conference on machine learning*, 8748–8763. PMLR.

Radford, A.; Narasimhan, K.; Salimans, T.; Sutskever, I.; et al. 2018. Improving language understanding by generative pre-training.

Radford, A.; Wu, J.; Child, R.; Luan, D.; Amodei, D.; Sutskever, I.; et al. 2019. Language models are unsupervised multitask learners. *OpenAI blog*, 1(8): 9.

Sariyildiz, M. B.; Perez, J.; and Larlus, D. 2020. Learning visual representations with caption annotations. In *Computer Vision—ECCV 2020: 16th European Conference, Glasgow, UK, August 23–28, 2020, Proceedings, Part VIII 16*, 153–170. Springer.

Soomro, K.; Zamir, A. R.; and Shah, M. 2012. UCF101: A dataset of 101 human actions classes from videos in the wild. *arXiv preprint arXiv:1212.0402*.

Xiao, J.; Hays, J.; Ehinger, K. A.; Oliva, A.; and Torralba, A. 2010. Sun database: Large-scale scene recognition from abbey to zoo. In *2010 IEEE computer society conference on computer vision and pattern recognition*, 3485–3492. IEEE.

Zhang, S.; Roller, S.; Goyal, N.; Artetxe, M.; Chen, M.; Chen, S.; Dewan, C.; Diab, M.; Li, X.; Lin, X. V.; et al. 2022. Opt: Open pre-trained transformer language models. *arXiv preprint arXiv:2205.01068*.

Zhou, K.; Yang, J.; Loy, C. C.; and Liu, Z. 2022a. Conditional prompt learning for vision-language models. In *Proceedings of the IEEE/CVF Conference on Computer Vision and Pattern Recognition*, 16816–16825.

Zhou, K.; Yang, J.; Loy, C. C.; and Liu, Z. 2022b. Learning to prompt for vision-language models. *International Journal of Computer Vision*, 130(9): 2337–2348.